



The Synergistic Effect of Biosynthesized Copper Oxide Nanoparticles and Vancomycin on Biofilm Formation of *Staphylococcus haemolyticus*

Zahraa M. Romi^{1*}   and Mais E. Ahmed²  

^{1,2}Department of Biology, College of Science, University of Baghdad, Baghdad, Iraq

*Corresponding Author.

Received: 21 March 2023

Accepted: 30 April 2023

Published: 20 April 2024

doi.org/10.30526/37.2.3374

Abstract

The results indicated that the biofilm formed by each *Staphylococcus haemolyticus* isolate was inhibited by 52%–82%. The highest value of biofilm formation (before treatment) was seen in the case of isolate A39, followed by A49 with absorption values of (1.382 and 1.116), respectively. Bacterial cells are capable of catalyzing the biosynthesis process by producing reductive enzymes. These green synthesized inorganic nanoparticles have been frequently investigated as possible bactericidal agents. Our findings revealed that at sub-Minimum Inhibitory Concentration (Sub-MIC), Copper oxide nanoparticles and Vancomycin combinations showed remarkable biofilm inhibitory outcomes in wild-type strains of *Staphylococcus haemolyticus* that are multidrug resistant. Strong biofilm producer strains were incubated with 100 μ l of sub-MIC synergistic nanoparticles for 24 h at 37 °C; the same strains showed weak biofilm production after incubation. This study was aimed at exploring whether synergistic green synthesized copper oxide nanoparticles and vancomycin combination can function as an anti-biofilm agent against *Staphylococcus haemolyticus* biofilm.

Keywords: Green synthesis, anti-biofilm, CuONps, biofilm.

1. Introduction

Applications of biological, physical, and chemical systems with dimensions ranging from single atoms or molecules to submicron dimensions are included in nanotechnology, along with nanoparticle manufacturing as well as their incorporation into larger systems. Three different methods are available for creating nanoparticles. They are as follows: The use of biological, physical, and chemical approaches [1] offers a range of options for achieving desired outcomes. The production of nanoparticles through biological processes is a relatively reliable alternative to more sophisticated chemical synthetic processes. In addition, the biosynthetic route (which utilizes fungi, algae, bacteria, plants, and other organisms as precursors) is gaining traction due to its capacity to overcome toxicity [2]. Cu NPs have great interest due to a variety of factors, including their affordability, ease of availability, and properties similar to those of noble metals [3]. *S. haemolyticus* is a gram-positive, facultatively anaerobic, non-spore-forming, and non-motile bacteria. *S. haemolyticus* is a type of coagulase-negative *staphylococcus* (CoNS) that lives on the skin. It is more strongly associated with opportunistic infections in immunocompromised individuals, especially those who are hospitalized and have medical implants worldwide [4].

After *S. epidermidis*, is the most typical CoNS to be isolated from blood cultures. The most



antibiotic-resistant *S. haemolyticus* isolates are found in nosocomial environments, but little is known about other factors contributing to the change from a "benign" skin commensal to an invasive lifestyle [5]. The ability of CoNS to adhere to polymer surfaces and the resulting biofilm formation are the main virulence factors [6]. Bacterial communities that are organized into aggregates and encased in an extracellular matrix are known as biofilms (ECM) [7]. A key component of *Staphylococcus* spp. has been identified as polysaccharide intercellular adhesin (PIA) [8]. The functionality of the biofilm is significantly influenced by its thickness and chemical composition. A thicker biofilm may make it more difficult for antibiotics to cross the barrier and reach bacterial cells because the polymer matrix specifically functions as a barrier and limits or prevents the diffusion of antibiotics [9]. Multidrug-resistant bacteria, including those responsible for *Staphylococcus*-related infections, are emerging in hospital-associated illnesses due to incorrect administration of antibiotics, including dosages, types, and durations [10]. *S. haemolyticus* has a flexible genome that facilitates the ability to survive against antimicrobial agents and can spread to other *Staphylococcus* group species [11]. Vancomycin has long been regarded as the first-line antibiotic for treating severe infections caused by methicillin-resistant CoNS. Vancomycin heteroresistance has, however, developed in these species as a result of increased usage of this antibiotic because of a wide range of complex molecular pathways, phenotypic instability, fluctuating vancomycin selection pressure, and insufficient genetic markers to make precise detections [12].

2. Materials and Methods

2.1. Collection and Identification of *S. haemolyticus* isolates

One hundred and fifty urine and seminal Fluid Samples were collected and mannitol salt agar and blood agar were used to culture the bacteria, which were then incubated for 24-48 hours at 37°C under aerobic conditions, suspected colonies were identified morphologically and biochemically [13]. Isolates were subsequently confirmed as *S. haemolyticus* by using the Vitek 2 compact system (bioMérieux France), following the instructions provided by the manufacturer. Plant material and experimental design.

2.2. Suspension of *S. haemolyticus*

Bacteria were cultured in Mueller Hinton Broth to prepare a suspension that was incubated for 18 h at 37°C. The bacteria were centrifuged for 10 minutes at 10,000 g at 4 °C. After removing the precipitate, we collected the supernatant to synthesize copper nanoparticles [14].

2.3. Biosynthesis of Copper oxide Nanoparticles

For the green synthesis of CuONps, 100 ml of deionized water was used to dissolve 0.1 M of copper acetate. A volume of 15 ml of 1mM copper acetate was added to 15 ml of *S. haemolyticus* supernatant after centrifugation and removal of the bacterial cell precipitate. The suspension was used to synthesize CuONps in 100 ml Erlenmeyer flasks. The flasks were incubated at 30 °C–35 °C, and any color change was recorded. Only the copper acetate was employed as a negative control, and no color change was observed over time [15].

2.4. Characterization of biosynthesized CuONPS

2.4.1. Suspension of *S. haemolyticus*

Bacteria were cultured in Mueller Hinton Broth to prepare a suspension that was incubated for 18 h at 37 ° C. The bacteria were centrifuged for 10 min at 10,000 g at 4 °C. After removing the precipitate, the supernatant was collected to synthesize copper nanoparticles [14].

2.4.2. Biosynthesis of Copper oxide Nanoparticles

For the green synthesis of CuONps, 100 ml of deionized water was used to dissolve 0.1 M of copper acetate. A volume of 15 ml of 1mM copper acetate was added to 15 ml of *S. haemolyticus* supernatant after centrifugation and removal of the bacterial cell precipitate. The suspension was used to synthesize CuONps in 100 ml Erlenmeyer flasks. The flasks were incubated at 30 °C–35 °C, and any color change was recorded. Only the copper acetate was employed as a negative control, and no color change was observed over time [15].

2.4.3. Characterization of biosynthesized CuONPS

Using the following techniques, the morphology and size of the CuONPs were investigated, such as atomic force microscopy (AFM), Energy dispersive X-ray (EDX), Field Emission Scanning Electron Microscopy (FESEM), Zeta Potential (ZP), and X-ray diffraction (XRD).

2.5. Biofilm activity of *S. haemolyticus*

Briefly, a sterile BHI was inoculated with 18-hour-old cultures of the selected strains at a final cell concentration of 1.5×10^8 CFU/ml. 180 µl of 1% glucose-containing brain heart infusion broth were added to sterile 96-well polystyrene microplates. Three sterile 96-well polystyrene microplates were filled with a volume of 20 µl of bacterial suspension. As a negative control, six wells containing brain heart infusion broth free of bacteria were taken into account. For 24 hours, the prepared plates were incubated at 37 °C to allow bacteria to form biofilms. The intensity of the biofilms was measured using a crystal violet assay after they were developed. The cultures were carefully discarded before being thoroughly washed with 1X PBS. Fix the adherent biofilms with 150 µl of methanol for 15 minutes and discard the excess. After 10 minutes of drying at room temperature, the plates were dyed for 15 minutes with 250 µl of a 0.2% (w/v) crystal violet solution. After rinsing off any excess crystal violet with distilled water, the plates were left to air dry for 30 minutes. 95% ethanol (v/v) was used to dissolve the adhered CV from the biofilms, which were then incubated for 15 minutes to read absorbance at OD 630 nm [16].

2.6. Determination of minimum Inhibition Concentration (MIC) of Vancomycin and CuONPs

Vancomycin and CuONPs antibacterial activity were evaluated for *S. haemolyticus* using the broth microdilution method [17]. Each Vancomycin (512 g/ml stock solution) was serially diluted twice, and in 1 ml of Muller Hinton broth, CuONPs (512 g/ml stock solution) were made with concentrations ranging from 64 to 2 g/ml. *S. haemolyticus* isolates were inoculated into nutrient broth and cultured at 37 °C for 24 hours. Vancomycin and CuONPS dilutions were transferred to microplate wells and inoculated with a bacterial sample with a turbidity of 0.5 McFarland standard. MHB medium was used as a negative control, while bacterial suspension with any addition was utilized as a positive control. For 24 hours, the microplate was incubated at 37°C. Then, in each well, bacterial growth was examined, and the minimum concentration that prevented noticeable growth was considered the MIC. In accordance with CLSI 2023 [18] guidelines, the MIC of vancomycin for each isolate was calculated.

2.7. Screening for antibiofilm activity of CuO NPs and vancomycin combination

The synergistic effect of sub-MIC Vancomycin and CuONPs was tested against biofilm action by using a modified method for the microtitre plate assay [19]. A 10ml of brain-heart infusion was incubated with bacteria for 24 hours at 37°C.

After which, using Densicheck, the cultures were diluted to 1.5×10^8 CFU/ml. To each well of the microplate, 100 µl of sub-MIC-concentrated CuONPs plus vancomycin solution combination and brain heart infusion broth were used to dilute that supplement with 1% glucose, then 100 µl

of bacterial solution were added. The final volume was 200 μ l per well. As a control, we used only the sterile liquid medium. The formed biofilm was measured by crystal violet after microplates were incubated at 37 $^{\circ}$ C for 24 hours, as described previously [16]. The following formula was used to determine the biofilm inhibition activity by using a multi-plate reader that was used to measure the optical density at 630 nm [20].

$$\% \text{ biofilm inhibition} = (\text{OD of untreated isolate} - \text{OD of treated isolate}) / \text{OD of untreated isolate} * 100$$

3. Results and Discussion

3.1. Identification of *S. haemolyticus*

We identified only 60 isolates of *S. haemolyticus*. Smaller than the characteristic yellow pinhead colonies of *S. aureus*, the colonies exhibited variable reactions on mannitol salt agar. Some strains displayed a positive reaction with yellow colonies, while others displayed a negative reaction with whitish pink non-fermentor ones [21]. While the isolates on blood agar displayed complete hemolysis in yellow-gray colonies that are (4–3) mm in diameter.

3.2. Determination of biofilm formation before CuONPs treatment

Microtiter plates were used to assess *S. haemolyticus* isolates (n = 55) for their ability to form biofilms quantitatively (MTP). The results demonstrated that isolates of *S. haemolyticus* biofilm production are 1(1.7%) non-producer, 17(30.3%) isolates produce weak biofilm, 29(51.7%) isolate moderate biofilm, and 8(14.5%) isolates are strong biofilm producers, as shown in **Figure 1**. Almost all *S. haemolyticus* isolates were biofilm producers. These results are compatible with the local study by [22], which concludes that the bacteria are capable of producing a strong biofilm. Also, in line with the Alhusain *et al.* [23] study, which revealed that all the isolates of *S. haemolyticus* were capable of yielding biofilm, one of which displayed a high accumulation of biofilm (O.D 0.7). The study is also quite similar to a study by [24], who found that (74%) of the *S. haemolyticus* isolates that have been tested could produce biofilms. The results contradict a previous study reported by [25], which revealed that 15% of the isolates formed strong biofilm, 6% produced moderate biofilm, 14% produced weak biofilm, and 66% produced no biofilm. The influence of different culture media, pH, temperature, and osmotic pressure could be attributed to variations in biofilm development caused by the presence of associated genes and different phenotypic methods. Stress and host immune system chemicals may play a role in discrepancies between biofilm production *in vivo* and *in vitro* [26]. As these organisms can colonize both abiotic and biotic surfaces, Biofilm formation is frequently associated with CoNS infections [27].

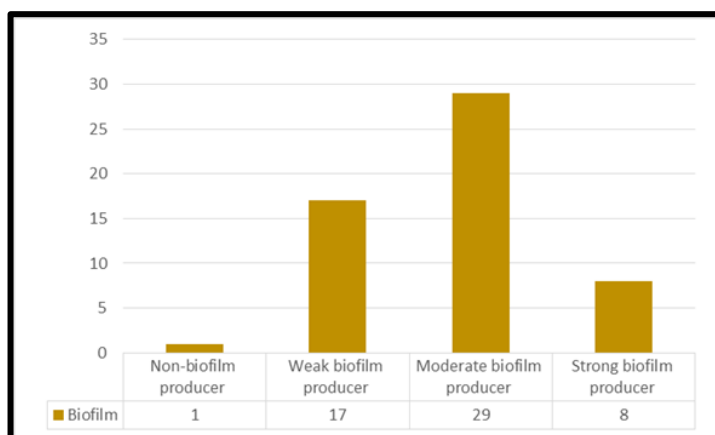


Figure 1. Percentage of biofilm values of *S. haemolyticus* isolates by Microtiter plate method.

3.3. Biosynthesis of Copper Oxide Nanoparticles:

Copper oxide nanoparticles were produced biologically from *S. haemolyticus*. A yellow-to-blue color change and the production of a light blue precipitate were indicators of the formation of nanoparticles. After centrifugation, the precipitate was greenish blue, and after microwave drying, we obtained a shiny blue powder as shown in **Figure 2**.

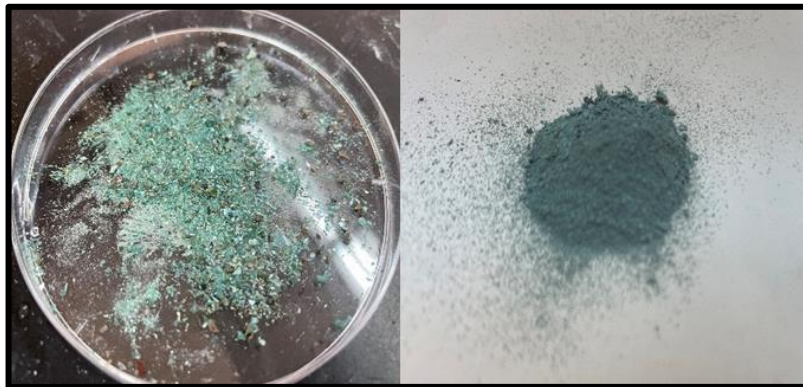


Figure 2. Biosynthesis of CuO Nanoparticles by *S. haemolyticus*.

In recent years, an obvious coordination to use bacteria to synthesize nanomaterials (mainly silver, zinc, gold, and copper) with remarkable properties has been observed in order to develop antimicrobials with in vitro activities against pathogenic bacteria other than antibiotics [28]. In recent years, it has been clear that scientists are collaborating to use bacteria to create nanomaterials (mostly silver, zinc, gold, and copper) with remarkable properties in order to create antimicrobials with in vitro actions against pathogenic bacteria other than antibiotics [29]. Bacteria are easy-cultivating microorganisms with short generation times; these characteristics make bacteria an ideal source for nanoparticle synthesis as they have extra cellular reduction enzymes [30]. Several bacterial types, such as *Escherichia coli*, *Pseudomonas fluoresces*, *Serratia sp.*, and *Pseudomonas stutzeri*, approved of their ability to reduce certain metal ions and produce nanoparticles [31].

3.4. Characterization of CuONPs

3.4.1. UV–Vis Spectral Analysis

The first method to characterize the copper oxide nanoparticles was UV-Vis spectrophotometry. The findings revealed that the maximum absorption peak of the biosynthesized CuONPs was 275 nm **Figure 3**.

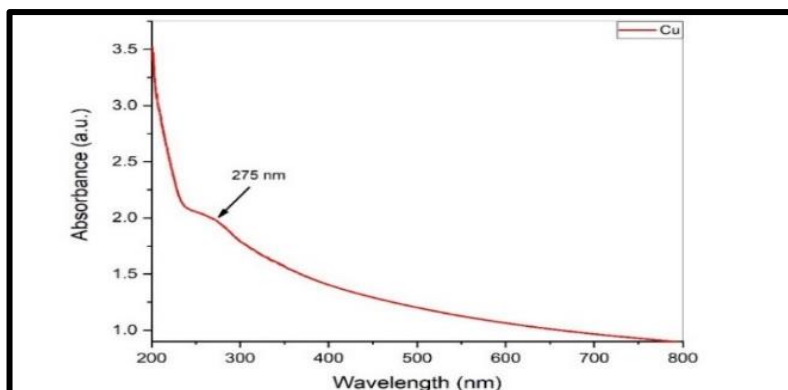


Figure 3. UV–Vis Spectrophotometry of CuONPs.

UV-visible spectroscopy analysis confirmed the bio-reduction of copper acetate to CuONPs as surface plasmon resonance (SPR) peaks. The CuONPs' surface plasmon band is characterized by SPR peaks. This agrees with a study by [32], which showed that the absorbance peak of copper nanoparticles was in the range of 250–360 nm. Another study by [33] recorded UV-Vis absorption spectra with peaks in the narrow absorbance range of 272–275 nm.

3.4.2. Atomic Force Microscopy (AFM) analysis

The size and surface morphology of CuONPs nanoparticles were determined using atomic force microscopy (AFM). The average size of biosynthesized CuONPS by *S. haemolyticus* according to **Figure 4**, is 35.48 nm. AFM analysis was used to identify and characterize bimodal nanoparticle distributions in CuONPs. The AFM results in this study are consistent with the AFM analysis of copper oxide nanoparticles generated using *Streptomyces cyaneus* [34].

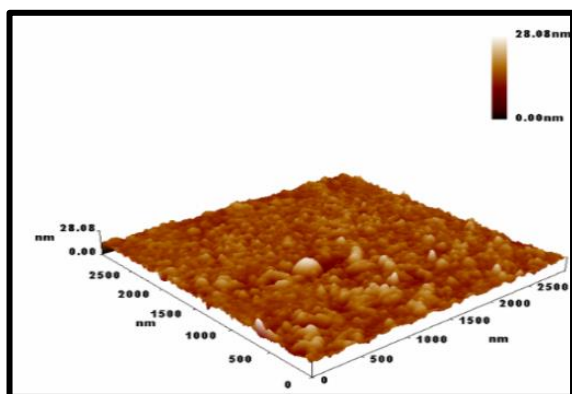


Figure 4. Three-dimensional image (3D) of CuONPs.

3.4.3. Field emission Scanning Electron Microscope (FESEM) and Energy dispersive X-ray (EDX)

The elemental and structural composition of NPs samples, as well as their morphology and size, were all examined using SEM analysis. **Figure 5a**, shows the spherical shape of CuONPs at 3000 kV and 40000 magnification power. According to SEM images, the diameter ranges from 15 to 19 nm, and the appearance is essentially spherical and uniform. Scanning electron microscopy was used to examine the morphology of the prepared nanoparticles. [35] study, reveals that copper oxide nanoparticles of spherical shape with diameters ranging from 24-99 nm and an average size of 77 nm show less aggregation. Which is in line with our findings. In comparison with an EDX-ray, FESEM allows for determining the presence of different components in the examined model.

Since copper (Cu) was obtained in the largest amount, it was clear from the EDX analysis that the synthesized CuONPs were pure **Figure 5b**. It reveals that the Cu content was 55.47 wt%, which proves the produced nanoparticles were in the purest form with small impurities. EDX provided both qualitative and quantitative examinations of elements that could be involved in nanoparticle production [36]. The results showed the EDX spectra together with the major elemental peak, specific to the Cu metal at 8 keV, and the composition percentage. Additional minor peaks for *S. haemolyticus* biomolecules were detected [37].

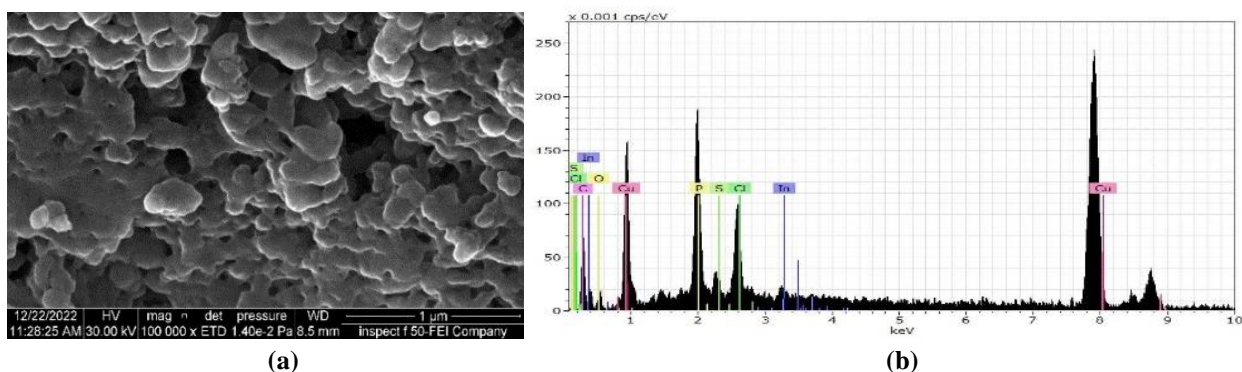


Figure 5. a) FE-SEM image of CuONPs b) Energy dispersive X-ray spectrometry of CuONPs.

3.4.5. Zeta potential (ZP)

It may be concluded that the biologically produced CuONPs are remarkably stable based on Figure 6, which displays the zeta potential of the CuONPs in this work to be -22.47 mV. Zeta potential is considered to be an important indication of a colloid's internal stability. According to electrokinetic potential, stability is classified as highly unstable between zeta values of ± 0 and ± 10 mV, generally stable between zeta values of ± 10 and ± 20 mV, moderately stable between zeta values of ± 20 and ± 30 mV, and highly stable beyond ± 30 mV. Which indicated that the synthesized NPs were remarkably stable and well-dispersed [38].

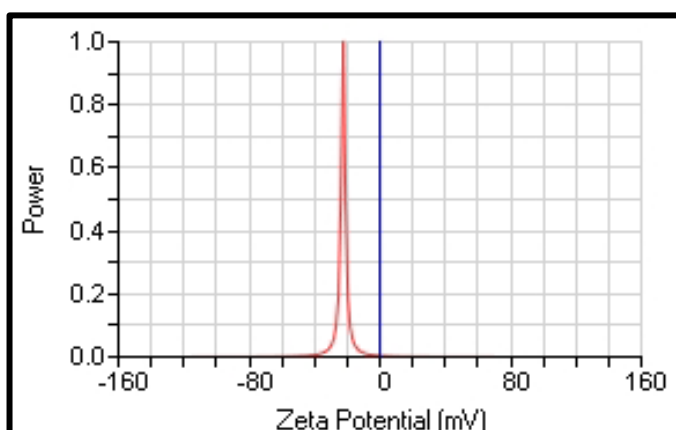


Figure 6. Zeta potential of CuONPs.

3.5. Minimum inhibitory concentration of Vancomycin and CuONPs

The MICs of vancomycin and CuONPs for the strongest biofilm producer *S. haemolyticus* isolates were determined in **Table 1**. The MIC value of vancomycin was $4 \mu\text{g/ml}$ for the seven isolates, indicating that all isolates are sensitive to vancomycin. While only one isolate was resistant to vancomycin with a MIC value of $32 \mu\text{g/ml}$, according to CLSI 2023 [18], The MIC of CuONPs was $4 \mu\text{g/ml}$ for A25, A37, A39, and A45. While the MIC of CuONPs against other isolates (A27, A35, A49, and A56) was $8 \mu\text{g/ml}$, CuONPs and vancomycin concentrations (64 , 32 , 16 , 8 , 4 , and 2) $\mu\text{g/ml}$ were introduced into each well. The outcome indicated different MIC concentrations. The CuONPs and vancomycin concentrations regarded as MICs are those where no detectable growth is observed. CuONPs have shown antibacterial activity against a variety of multidrug-resistant bacterium species, including clinical isolates of *S. aureus* and *E. coli* [39]. The results are in excellent agreement with previous studies demonstrating the minimum inhibitory concentration of CuONPs [40, 41]. The results of the Ramzan *et al.*[42] investigation

demonstrated that gram-positive bacteria are sensitive to the greenly produced copper oxide nanoparticles at concentrations between 25 and 150 $\mu\text{g/ml}$. Recently, a study by Raju *et al.* [43] documented that the MIC values of CuONPs were 12.5 $\mu\text{g/ml}$ and 10 $\mu\text{g/ml}$ for the gram-positive bacteria *S. aureus*, respectively. The previous research points to various pathways for metallic NPs' antibacterial activity. CuONPs are thought to interact with bacterial cell walls related to their large surface areas, which contributes to their high reactivation [44]. Especially, the electrical interactions produced by CuONPs with smaller sizes and larger surface areas increased the NPs' surface responsiveness. Additionally, the bacterium immediately engages with the increased surface area percentage, improving bacterial interaction throughout the process. These two essential elements (Cu and O in NPs) significantly increase the antibacterial activity of NPs with a large surface area [45]. When suspended in aqueous solutions, copper nanoparticles with reactive surfaces have been found to produce reactive oxygen species (ROS) [46]. Exposure to CuO NPs and the subsequent release of reactive oxygen species (ROS) would result in the generation of superoxide species, which would facilitate the subsequent destruction of biomolecules (lipid peroxidation and protein oxidation) [47].

Table 1. The minimal inhibitory concentration of vancomycin and CuONPs

Bacterial isolate NO.	A25	A27	A35	A37	A39	A45	A49	A56
MIC of Vancomycin ($\mu\text{g/ml}$)	4	4	32	4	4	4	4	4
MIC of CuONPs ($\mu\text{g/ml}$)	4	8	8	4	4	4	8	8

3.6. Antibiofilm activity of Sub-MIC of Vancomycin and CuONPs combination

The biofilm mass of each isolate was reduced from strong to weak. We observed that the biofilm formed by each of the strongest biofilm producers, *S. haemolyticus* isolates, was inhibited with a (52-82) percentage in **Table 2**. The highest value of biofilm formation (before treatment) was seen in the case of isolate A39, followed by A49 with absorption values of 1.382 and 1.116, respectively. After treatment with vancomycin and CuONPs combination, there was a decrease in biofilm formation in the cases of A39 and A49 isolates with absorbency values (0.295 and 0.318), respectively.

Table 2. Antibiofilm activity of Sub MIC of Vancomycin and CuONPs.

Bacterial isolate NO.	O.D before treatment	O.D after treatment	Percentage of inhibition
A30	0.773	0.141	82%
A39	1.382	0.295	79%
A49	1.116	0.318	76%
A45	1.013	0.327	68%
A56	1.1	0.361	67%
A25	0.665	0.29	56%
A37	0.765	0.359	54%
A35	0.56	0.274	52%

Biofilm production was significantly reduced after 24 hours of incubation at 37°C with Sub-MIC of vancomycin and CuONPs combination, OD measurement of the same isolates of *S. haemolyticus* decreased from strong to weak production. These findings are similar to [48] study, which stated that biofilm development decreased with increasing concentrations of CuONPs, with (1024 $\mu\text{g/ml}$) concentration showing the maximum inhibition and the (4 $\mu\text{g/ml}$) concentration showing the lowest inhibition. In the case of Staphylococci, "last-line" treatments, such as

vancomycin, are still available for treating infections caused by these pathogens. But some time, because of the high prevalence of these species in healthcare settings, there is a significant selective pressure for the generation of resistant clones, the increasing clinical use of these last-resort antimicrobials, and the capacity of these species to evolve antibiotic resistance. As a result, resistance to these last-line antibiotics has become more common, leading to treatment failure [49].

Therefore, the treatment of *S. haemolyticus* infections with combination therapy remains an area of active research interest. According to [50] CuONPs were found to significantly reduce the formation of biofilm on surfaces coated with them, which could be attributable to their inhibitory effect on bacterial adherence.

Because smaller particles have a greater surface area for interacting with microorganisms than the bacterial control, CuONPs have a greater influence on biofilm inhibition. Copper ions have the ability to prevent bacterial growth and development by rupturing the bacterial cell wall or cell membrane. They will interact with phosphorus- and sulfur-rich molecules like DNA once inside the cell due to their affinity for them [51]. These events might trigger a series of redox reactions that would generate reactive oxygen species, disrupt bacterial membranes, and result in oxidative stress and cell death [52].

4. Conclusion

Copper oxide nanoparticles demonstrated promising antibacterial and antibiofilm activity. Vancomycin had MICs of 2 µg/ml against the seven strongest biofilm producers, *S. haemolyticus* isolates, except one isolate was resistant with a MIC of 32 µg/ml. While CuONPs had MICs of 4 and 8 µg/ml against the strongest biofilm producers, *S. haemolyticus* isolates, CuONPs and vancomycin Sub-MIC were very effective in dislodging preformed biofilms. The antibiofilm potential was extremely encouraging (80 % inhibition against A30 *S. haemolyticus* isolate).

Acknowledgment

Many thanks to editor-in-chief and members of the editorial committee in Ibn Al-Haitham Journal for Pure and Applied Sciences.

Conflict of Interest

There are no conflicts of interest.

Funding

There is no funding for the article.

References

1. Saleh, G. M.; Shaymaa S. N. Antibacterial Activity of Silver Nanoparticles Synthesized from Plant Latex. *Iraqi Journal of Science* **2020**, 1579–1588. DOI: <https://doi.org/10.24996/ij.s.2020.61.7.5>.
2. Alao, I.I.; Oyekunle, I.P.; Iwuozor, K.O.; Emenike, E.C. Green Synthesis of Copper Nanoparticles and Investigation of Its Antimicrobial Properties. *Advanced Journal of Chemistry-Section B: Natural Products and Medical Chemistry* **2022**, 4, 39–52. DOI: <https://doi.org/10.22034/ajcb.2022.323779.1106>.
3. Hasanin, M.; Al Abboud, M.A.; Alawlaqi, M.M.; Abdelghany, T.M.; Hashem, A.H. Ecofriendly Synthesis of Biosynthesized Copper Nanoparticles with Starch-Based Nanocomposite: Antimicrobial, Antioxidant, and Anticancer Activities. *Biol. Trace Elem. Res* **2022**, 200, 2099–2112.

- DOI: <https://doi.org/10.1007/s12011-021-02812-0>.
4. Eltwisy, H.O.; Twisy, H.O.; Hafez, M.H.; Sayed, I.M.; El-Mokhtar, M.A. Clinical Infections, Antibiotic Resistance, and Pathogenesis of *Staphylococcus haemolyticus*. *Microorganisms* **2022**, *10*, 1130. DOI: <https://doi.org/10.3390/microorganisms10061130>.
 5. Cavanagh, J.P.; Pain, M.; Askarian, F.; Bruun, J.-A.; Urbarova, I.; Wai, S.N.; Schmidt, F.; Johannessen, M. Comparative Exoproteome Profiling of an Invasive and a Commensal *Staphylococcus haemolyticus* Isolate. *J. Proteomics* **2019**, *197*, 106–114, DOI: [10.1016/j.jprot.2018.11.013](https://doi.org/10.1016/j.jprot.2018.11.013).
 6. Nandan, P.; Sharan, S. Prospective Observational Research to Determine Antimicrobial Susceptibility and Biofilm Production among Coagulase Negative Staphylococci. *International Journal of Pharmaceutical and Clinical Research* **2022**, *14*, 666–671. <https://impactfactor.org/PDF/IJPCR/14/IJPCR,Vol14,Issue1,Article99.pdf>
 7. Azulay, D.N.; Spaeker, O.; Ghrayeb, M.; Wilsch-Bräuninger, M.; Scoppola, E.; Burghammer, M.; Zizak, I.; Bertinetti, L.; Politi, Y.; Chai, L. Multiscale X-Ray Study of *Bacillus subtilis* Biofilms Reveals Interlinked Structural Hierarchy and Elemental Heterogeneity. *Proc. Natl. Acad. Sci. U. S. A.* **2022**, *119*, e2118107119. DOI: <https://doi.org/10.1073/pnas.2118107119>.
 8. Rampelotto, R.F.; Lorenzoni, V.V.; Silva, D. da C.; Coelho, S.S.; Wust, V.; Garzon, L.R.; Nunes, M.S.; Meneghetti, B.; Brites, P.C.; Hörner, M.; et al. Assessment of Different Methods for the Detection of Biofilm Production in Coagulase-Negative Staphylococci Isolated from Blood Cultures of Newborns. *Rev. Soc. Bras. Med. Trop* **2018**, *51*, 761–767. DOI: <https://doi.org/10.1590/0037-8682-0171-2018>.
 9. Goetz, C.; Tremblay, Y.D.N.; Lamarche, D.; Blondeau, A.; Gaudreau, A.M.; Labrie, J.; Malouin, F.; Jacques, M. Coagulase-Negative Staphylococci Species Affect Biofilm Formation of Other Coagulase-Negative and Coagulase-Positive Staphylococci. *J. Dairy Sci.* **2017**, *100*, 6454–6464. DOI: <https://doi.org/10.3168/jds.2017-12629>.
 10. Suhartono; Hayati, Z.; Mahmuda Distribution of *Staphylococcus Haemolyticus* as the Most Dominant Species among Staphylococcal Infections at the Zainoel Abidin Hospital in Aceh, Indonesia. *Biodiversitas* **2019**, *20*. DOI: <https://doi.org/10.13057/biodiv/d200739>
 11. Haliman, C.C.; Prasetyo, D.S.; Tjampakasari, C.R. Multidrug Resistance and Extensively Drug-Resistance in *Staphylococcus aureus*, *Staphylococcus epidermidis*, and *Staphylococcus haemolyticus*. *Microbiol Indones* **2022**, *16*. DOI: <https://doi.org/10.7324/JAPS.2022.120601>.
 12. Pereira-Ribeiro, P.M.A.; Cabral-Oliveira, G.G.; Olivella, J.G.B.; Motta, I.C. de M.; Ribeiro, F.C.; Nogueira, B.A.; Santos, L.S. dos; Sued-Karam, B.R.; Mattos-Guaraldi, A.L. Biofilm Formation, Multidrug-Resistance and Clinical Infections of *Staphylococcus haemolyticus*: A Brief Review. *Res. Soc. Dev.* **2022**, *11*, e228111133605. DOI: <https://doi.org/10.33448/rsd-v11i11.33605>.
 13. Nakamura, K.; O'Neill, A.M.; Williams, M.R.; Cau, L.; Nakatsuji, T.; Horswill, A.R.; Gallo, R.L. Short Chain Fatty Acids Produced by Cutibacterium Acnes Inhibit Biofilm Formation by *Staphylococcus epidermidis*. *Sci. Rep.* **2020**, *10*, 21237. DOI: <https://doi.org/10.1038/s41598-020-77790-9>.
 14. Schleifer, K.H.; Bell, J.A. *Staphylococcus*. *Bergey's Manual of Systematics of Archaea and Bacteria*. **2015**, 1–43.
 15. Shantkriti, S.; Rani, P. Biological Synthesis of Copper Nanoparticles Using *Pseudomonas fluorescens*. *Int J Curr Microbiol App Sci* **2014**, *3*, 374–383. <https://www.ijcmas.com/vol-3-9/S.Shantkriti%20and%20P.Rani.pdf>
 16. Stepanović, S.; Vuković, D.; Hola, V.; Di Bonaventura, G.; Djukić, S.; Cirković, I.; Ruzicka, F. Quantification of Biofilm in Microtiter Plates: Overview of Testing Conditions and Practical Recommendations for Assessment of Biofilm Production by Staphylococci. *APMIS* **2007**, *115*, 891–899. DOI: https://doi.org/10.1111/j.1600-0463.2007.apm_630.x.
 17. Mirzaei, R.; Alikhani, M.Y.; Arciola, C.R.; Sedighi, I.; Irajian, G.; Jamasbi, E.; Yousefimashouf, R.;

- Bagheri, K.P. Highly Synergistic Effects of Melittin with Vancomycin and Rifampin against Vancomycin and Rifampin Resistant *Staphylococcus epidermidis*. *Front. Microbiol.* **2022**, *13*, 869650. DOI: <https://doi.org/10.3389/fmicb.2022.869650>.
18. AST 2023 Available online: <https://clsi.org/ast-2023/> (accessed on 31 March 2023).
 19. Ben Abdallah, F.; Lagha, R.; Gaber, A. Biofilm Inhibition and Eradication Properties of Medicinal Plant Essential Oils against Methicillin-Resistant *Staphylococcus aureus* Clinical Isolates. *Pharmaceuticals (Basel)* **2020**, *13*, 369. DOI: <https://doi.org/10.3390/ph13110369>.
 20. Rima, M.; Trognon, J.; Latapie, L.; Chbani, A.; Roques, C.; El Garah, F. Seaweed Extracts: A Promising Source of Antibiofilm Agents with Distinct Mechanisms of Action against *Pseudomonas aeruginosa*. *Mar. Drugs* **2022**, *20*, 92. DOI: <https://doi.org/10.3390/md20020092>.
 21. Bouchami, O.; Machado, M.; Carriço, J.A.; Melo-Cristino, J.; de Lencastre, H.; Miragaia, M. Spontaneous Genomic Variation as a Survival Strategy of Nosocomial *S. haemolyticus*. *bioRxiv* **2022**. DOI: <https://doi.org/10.1101/2022.05.17.492267>.
 22. Al-Mousawi, A.H.; Al-Kaabi, S.J.; Mic, S.-.; Mic, S.; Mic, S.; Mic, S.-.; Mic, S.-.; Mic, S.-.; Mic, S.-.; Mic, S.-.; Mic, S.-. Effect of Ziziphus Spina Christy on Biofilm Formation of Methicillin Resistance *Staphylococcus aureus* and *Staphylococcus haemolyticus*. **2018**, *18*, 1033–1038. DOI: <https://doi.org/10.1155/2022/4495688>.
 23. Alhusain, M.T.A.; Jaafar, F.N.; Hassan, A.A.A. Isolation and Characterization of *Staphylococcus haemolyticus* from Urinary Tract Infection. *EurAsian Journal of BioSciences* **2020**, *14*, 1909–1913.
 24. Fredheim, E.G.A.; Klingenberg, C.; Rohde, H.; Frankenberger, S.; Gaustad, P.; Flaegstad, T.; Sollid, J.E. Biofilm Formation by *Staphylococcus haemolyticus*. *J. Clin. Microbiol.* **2009**, *47*, 1172–1180. DOI: <https://doi.org/10.1128/JCM.01891-08>.
 25. Silva, P.V.; Cruz, R.S.; Keim, L.S.; Paula, G.R.; Teixeira, B.; Carvalho, F.; Coelho, L.R.; Cícera, M.; Mauricio, J.; Marie, A.; et al. The Antimicrobial Susceptibility, Biofilm formation and genotypic profiles of *Staphylococcus haemolyticus* from bloodstream infections **2013**, *108*, 812–816. DOI: [10.1590/0074-0276108062013022](https://doi.org/10.1590/0074-0276108062013022).
 26. Pinheiro, L.; Ivo, C.; Oliveira, A.; Cataneli, V.; Lourdes, M.; Souza, R. *Staphylococcus Epidermidis* and *Staphylococcus Haemolyticus* : Detection of Biofilm Genes and Biofilm Formation in Blood Culture Isolates from Patients in a Brazilian Teaching Hospital. *Diagnostic Microbiology and Infectious Disease* **2016**, 1–4. DOI: <https://doi.org/10.1016/j.diagmicrobio.2016.06.006>.
 27. Silva, V.; Correia, E.; Pereira, J.E.; González-Machado, C.; Capita, R.; Alonso-Calleja, C.; Igrejas, G.; Poeta, P. Exploring the Biofilm Formation Capacity in *S. Pseudintermedius* and Coagulase-Negative Staphylococci Species. *Pathogens* **2022**, *11*. DOI: <https://doi.org/10.3390/pathogens11060689>.
 28. Eid, A.M.; Fouda, A.; Hassan, S.E.; Hamza, -D; Alharbi, M.F.; Elkelish, N.K.; Alharthi, A.; Salem, A. Plant-Based Copper Oxide Nanoparticles; Biosynthesis, Characterization, Antibacterial Activity, Tanning Wastewater Treatment, and Heavy Metals Sorption. **2023**, *13*. DOI: <https://doi.org/10.3390/catal13020348>.
 29. Kadhim, Z.H.; Ahmed, M.E.; Şimşek, I. The Synergistic Effect of Copper Nanoparticles and Vancomycin in Vitro and in Vivo. *Pakistan Journal of Medical and Health Sciences* **2022**, *16*, 594–59. DOI: <https://doi.org/10.53350/pjmhs22168594>.
 30. Rashid, A.E.; Ahmed, M.E.; Hamid, M.K. Evaluation of Antibacterial and Cytotoxicity Properties of Zinc Oxide Nanoparticles Synthesized by Precipitation Method against Methicillin-Resistant *Staphylococcus aureus*. *Int. J. Drug Deliv. Technol.* **2022**, *12*, 985–989. DOI: <https://doi.org/10.25258/ijddt.12.3.11>.
 31. Singh, J.; Dutta, T.; Kim, K.H.; Rawat, M.; Samddar, P.; Kumar, P. Green” Synthesis of Metals and Their Oxide Nanoparticles: Applications for Environmental Remediation. *Journal of Nanobiotechnology* **2018**, *16*, 1–24. DOI: <https://doi.org/10.1186/s12951-018-0408-4>.
 32. Raina, S.; Roy, A.; Bharadvaja, N. Degradation of Dyes Using Biologically Synthesized Silver and

- Copper Nanoparticles. *Environ. Nanotechnol. Monit. Manag.* **2020**, *13*, 100278. DOI: <https://doi.org/10.1016/j.enmm.2019.100278>.
33. Ssekatawa, K.; Byarugaba, D.K.; Angwe, M.K.; Wampande, E.M.; Ejobi, F.; Nxumalo, E.; Maaza, M.; Sackey, J.; Kirabira, J.B. Phyto-Mediated Copper Oxide Nanoparticles for Antibacterial, Antioxidant and Photocatalytic Performances. *Front. Bioeng. Biotechnol.* **2022**, *10*, 820218. DOI: <https://doi.org/10.3389/fbioe.2022.820218>.
 34. Waris, A.; Din, M.; Ali, A.; Ali, M.; Afridi, S.; Baset, A.; Ullah Khan, A. A Comprehensive Review of Green Synthesis of Copper Oxide Nanoparticles and Their Diverse Biomedical Applications. *Inorg. Chem. Commun.* **2021**, *123*, 108369. DOI: <https://doi.org/10.1016/j.inoche.2020.108369>.
 35. Kouhkan, M.; Ahangar, P.; Babaganjeh, L.A.; Allahyari-Devin, M. Biosynthesis of Copper Oxide Nanoparticles Using *Lactobacillus casei* Subsp. *casei* and Its Anticancer and Antibacterial Activities. *Curr. Nanosci.* **2020**, *16*, 101–111. DOI: <https://doi.org/10.2174/1573413715666190318155801>.
 36. Amaliyah, S.; Pangesti, D.P.; Masruri, M.; Sabarudin, A.; Sumitro, S.B. Green Synthesis and Characterization of Copper Nanoparticles Using Piper Retrofractum Vahl Extract as Bioreductor and Capping Agent. *Heliyon* **2020**, *6*, e04636. DOI: <https://doi.org/10.1016/j.heliyon.2020.e04636>.
 37. Ghosh, M.K.; Sahu, S.; Gupta, I.; Ghorai, T.K. Green Synthesis of Copper Nanoparticles from an Extract of Jatropha Curcasleaves: Characterization, Optical Properties, CT-DNA Binding and Photocatalytic Activity. *RSC Advances* **2020**, *10*, 22027–22035. DOI: <https://doi.org/10.1039/D0RA03186K>.
 38. Atiya, M. A.; Hassan, A. K.; Kadhim, F. Q. Green synthesis of copper nanoparticles using tea leaves extract to remove ciprofloxacin (CIP) from aqueous media. *Iraqi Journal of Science* **2021**, *62*, 2833–2854. DOI: <https://doi.org/10.24996/ij.s.2021.62.9.1>.
 39. Ameh, T.; Zarzosa, K.; Dickinson, J.; Braswell, W.E.; Sayes, C.M. Nanoparticle Surface Stabilizing Agents Influence Antibacterial Action. *Front. Microbiol.* **2023**, *14*, 1119550. DOI: <https://doi.org/10.3389/fmicb.2023.1119550>.
 40. Amiri, M.; Etemadifar, Z.; Daneshkazemi, A.; Nateghi, M. Antimicrobial Effect of Copper Oxide Nanoparticles on Some Oral Bacteria and Candida Species. *J. Dent. Biomater.* **2017**, *4*, 347–352. DOI: <https://pubmed.ncbi.nlm.nih.gov/28959764/>.
 41. Dlamini, N.G.; Basson, A.K.; Pullabhotla, V.S.R. Optimization and Application of Bioflocculant Passivated Copper Nanoparticles in the Wastewater Treatment. *Int. J. Environ. Res. Public Health* **2019**, *16*, 2185. DOI: <https://doi.org/10.3390/ijerph16122185>.
 42. Ramzan, M.; Obodo, R.M.; Mukhtar, S.; Ilyas, S.Z.; Aziz, F.; Thovhogi, N. Green Synthesis of Copper Oxide Nanoparticles Using Cedrus Deodara Aqueous Extract for Antibacterial Activity. *Mater. Today* **2021**, *36*, 576–581. DOI: <https://doi.org/10.1016/j.matpr.2020.05.472>.
 43. Raju, S.K.; Sekar, P.; Kumar, S.; Sundhararajan, N.; Nagalingam, Y. Green Synthesis and Antimicrobial Evaluation of Copper Oxide Nanoparticles Derived from Aqueous Leaves Extract of Indigofera Cassioides Rottl. *Ex. Journal of Xidian University* **2023**, *17*. DOI: [10.37896/jxu17.2/012](https://doi.org/10.37896/jxu17.2/012).
 44. Vasantharaj, S.; Sathiyavimal, S.; Saravanan, M.; Senthilkumar, P.; Gnanasekaran, K.; Shanmugavel, M.; Manikandan, E.; Pugazhendhi, A. Synthesis of Ecofriendly Copper Oxide Nanoparticles for Fabrication over Textile Fabrics: Characterization of Antibacterial Activity and Dye Degradation Potential. *J. Photochem. Photobiol. B* **2019**, *191*, 143–149. DOI: <https://doi.org/10.1016/j.jphotobiol.2018.12.026>.
 45. Rajamohan, R.; Raorane, C.J.; Kim, S.-C.; Lee, Y.R. One Pot Synthesis of Copper Oxide Nanoparticles for Efficient Antibacterial Activity. *Materials (Basel)* **2022**, *16*, 217. DOI: <https://doi.org/10.3390/ma16010217>.
 46. Qamar, H.; Rehman, S.; Chauhan, D.K.; Tiwari, A.K.; Upmanyu, V. Green Synthesis, Characterization and Antimicrobial Activity of Copper Oxide Nanomaterial Derived from Momordica Charantia. *Int. J. Nanomedicine* **2020**, *15*, 2541–2553. DOI: <https://doi.org/10.2147/IJN.S240232>.

47. Raheem, H.Q.; Al-meamar, T.S.; Almamoori, A.M. Antibiotic Profile And Antibacterial Activity Of Copper Oxide Nanoparticles Against *Pseudomonas fluorescens* Isolated From Wound Infection. *Int. J. Drug Deliv. Technol.* **2019**, *9*. DOI: <https://doi.org/10.25258/ijddt.v9i3.10>.
48. Mohamed, A.H.; Kadium, S. Biological Effect of Copper Oxide Nanoparticles Synthesized by *Saccharomyces boulardii* against of Multidrug Resistant Bacteria Isolated from Diabetic Foot Infections. *Cardiometry* **2022**, *25*, 31–40. DOI: <https://doi.org/10.18137/cardiometry.2022.25.3140>.
49. Turner, A.M.; Lee, J.Y.H.; Gorrie, C.L.; Howden, B.P.; Carter, G.P. Genomic Insights into Last-Line Antimicrobial Resistance in Multidrug-Resistant *Staphylococcus* and Vancomycin-Resistant *Enterococcus*. *Front. Microbiol.* **2021**, *12*, 637656. DOI: <https://doi.org/10.3389/fmicb.2021.637656>.
50. Hashemifard Dehkordi, P.; Moshtaghi, H.; Abbasvali, M.; Dehkordi, K.R. Effects of Magnesium Oxide and Copper Oxide Nanoparticles on Biofilm Formation of *Escherichia coli* and *Listeria monocytogenes*. *Nanotechnology* **2023**, *34*. DOI: <https://doi.org/10.1088/1361-6528/acab6f>.
51. Shehabeldine, A.M.; Amin, B.H.; Hagrass, F.A.; Ramadan, A.A.; Kamel, M.R.; Ahmed, M.A.; Atia, K.H.; Salem, S.S. Potential Antimicrobial and Antibiofilm Properties of Copper Oxide Nanoparticles: Time-Kill Kinetic Essay and Ultrastructure of Pathogenic Bacterial Cells. *Appl. Biochem. Biotechnol.* **2023**, *195*, 467–485. DOI: <https://doi.org/10.1007/s12010-022-04120-2>.
52. Cherian, T.; Ali, K.; Saquib, Q.; Faisal, M.; Wahab, R.; Musarrat, J. *Cymbopogon citratus* Functionalized Green Synthesis of CuO-Nanoparticles: Novel Prospects as Antibacterial and Antibiofilm Agents. *Biomolecules* **2020**, *10*, 169. DOI: <https://doi.org/10.3390/biom10020169>.